Inorg. Chem. **2004**, *43*, 5877–5883

Ultrasonic-Assisted Synthesis of Monodisperse Single-Crystalline Silver Nanoplates and Gold Nanorings

Li-Ping Jiang,[†] Shu Xu,[†] Jian-Min Zhu,[‡] Jian-Rong Zhang,[†] Jun-Jie Zhu,*[,†] and Hong-Yuan Chen[†]

Laboratory of Life Analytical Chemistry, Department of Chemistry, and National Laboratory of Solid State of Microstructures, Nanjing University, Nanjing 210093, People's Republic of China

Received April 10, 2004

A simple sonochemical route was developed for the crystal growth of uniform silver nanoplates and ringlike gold nanocrystals in a *N*,*N*-dimethylformamide solution. The platelike structures were generated from the selective growth on different crystal planes in the presence of poly(vinylpyrrolidone) and the ultrasonic-assisted Ostwald ripening processes. The silver nanoplates in solution served as the templates for the synthesis of ringlike gold crystals via a displacement reaction. Both the silver nanoplates and gold nanorings were highly oriented single crystals with (111) planes as the basal planes.

Introduction

Metal nanoparticles such as silver and gold have many important applications in many aspects such as the catalysis process,[1] optics,[2] surface-enhanced Raman spectroscopy,[3] etc. It is well-known that the physical, optical, and chemical properties of nanoparticles depend on their size and shape greatly. Especially for many nanosized metal and semiconductor materials, the two-dimensional (2D) structures such as nanoprisms,[4,5] nanoplates,[6−16] nanodisks,[17,18] and nanorings[7,19] are believed to have marvelous ability to control optical properties.

Therefore, it is very essential to develop a simple and effective preparation method of metal nanoparticles for well-controlled sizes and shapes. In recent years, much research and development has been focused on the growth and properties of silver nanoparticles with 2D structures.[4−6,8,14,17−18,20−22] Noble gold ringlike structures have also been prepared via a displacement reaction using a platelike structure as a template.[7,19] The processes in these approaches include the following: a photoinduced process,[4,7,14,20] a thermal process,[5−8,18,21−22] and a solution method at room temperature.[17,19] Here we report an ultrasonic-assisted approach to prepare silver platelike and gold ringlike structures. The ultrasonic irradiation offers a kinetic process different from these processes and can promise a very short reaction time and relatively stable reaction conditions which come from the enhanced Ostwild ripening processes. The ultrasonic-assisted process leads to more uniform silver nanoplates and gold nanorings.

The sonochemical method has been used extensively to generate novel nanostructed materials with unusual properties since 1934. The chemical effects of ultrasound arise from

* Author to whom correspondence should be addressed. E-mail: jjzhu@nju.edu.cn. Fax: +86-25-83317761. Phone: +86-25-83594976.
[†] Laboratory of Life Analytical Chemistry, Department of Chemistry.
[‡] National Laboratory of Solid State of Microstructures.

(1) El-sayed, M. A. *Acc. Chem. Res.* **2001**, *34*, 257.
(2) Eychmuller, A. *J. Phys. Chem. B* **2001**, *104*, 6514.
(3) Mirkin, C. A.; Lestinger, R. L.; Mucic, R. C.; Storhoff, J. J. *Nature* **1996**, *382*, 607.
(4) Jin, R. C.; Cao, Y. W.; Mirkin, C. A.; Kelly, K. L.; Schatz, G. C.; Zheng, J. G. *Science* **2001**, *294*, 1901.
(5) Pastoriza-Santos, I.; Liz-Marzan, L. M. *Nano Lett.* **2002**, *2*, 903.
(6) Sun, Y.; Mayers, B.; Xia, Y. *Nano Lett.* **2003**, *3*, 675.
(7) Sun, Y.; Xia, Y. *Adv. Mater.* **2003**, *15*, 695.
(8) Chen, S.; Carroll, D. L. *Nano Lett.* **2002**, *2*, 1003.
(9) Zhou, Y.; Wang, C. Y.; Zhu, Y. R.; Chen, Z. Y. *Chem. Mater.* **1999**, *11*, 2310.
(10) Curtis, A. C.; Duff, D. G.; Edwards, P. P.; Jefferson, D. A.; Johnson, B. F. G.; Kirkland, A.; Wallace, A. S. *Angew. Chem., Int. Ed. Engl.* **1988**, *27*, 1530.
(11) Bradley, J. S.; Tesche, B.; Busser, W.; Maase, M.; Reetz, M. T. *J. Am. Chem. Soc.* **2000**, *122*, 4631.
(12) Ibano, D.; Yokota, Y.; Tominaga, T. *Chem. Lett.* **2003**, *32*, 574.
(13) Tsuji, M.; Hashimoto, M.; Nishizawa, Y.; Tsuji, T. *Chem. Lett.* **2003**, *32*, 1114.
(14) Callegari, A.; Tonti, D.; Chergui, M. *Nano Lett.* **2003**, *3*, 1565.
(15) Yener, D. O.; Sindel, J.; Randall, C. A.; Adair, J. H. *Langmuir* **2002**, *18*, 8692.
(16) Khomutov, G. B.; Bykov, I. V.; Gainutdinov, R. V.; Gubin, S. P.; Obydenov, A. Y.; Polyakov, S. N.; Tolstikhina, A. L. *Colloids Surf., A: Physicochem. Eng. Aspects* **2002**, *198*, 347.
(17) Maillard, M.; Giorgio, S.; Pileni, M. P. *Adv. Mater.* **2002**, *14*, *15*, 1084.
(18) Hao, E.; Kelly, K. L.; Hupp, J. T.; Schatz; G. C. *J. Am. Chem. Soc.* **2002**, *124*, 15182.
(19) Metraux, G. S.; Cao, Y. C.; Jin, R.; Mirkin, C. A. *Nano Lett.* **2003**, *3*, 519.

10.1021/ic049529d CCC: $27.50
Published on Web 08/17/2004

acoustic cavitation, that is, the formation, growth, and implosive collapse of bubbles in a liquid. When solutions are exposed to strong ultrasound irradiation, bubbles in the solution are implosively collapsed by acoustic fields; as a result, the temperature can be as high as 5000 K, the pressure can reach over 1800 atm, and the cooling rate can be in excess of 10^6 K/s.[23−25] Cavitation bubble collapse can also induce a shock wave in the solution and drive rapid impact of the liquid to the surface of the particles. Thus, a lot of nanostructured materials[25,26] have been prepared via the sonochemical method.

In this study, monodisperse silver nanoplates have been prepared via a simple sonochemical route. The TEM observation and UV−vis spectral characterization described a clear ultrasonic-assisted Ostwald ripening process including the following stages: the formation of prism-like seeds from the initial 2−5 nm spherical particles which were synthesized through a reduction reaction; a rapid dissolution and growth process from seeds to larger crystals; a slow growth process from the larger crystals to uniform silver nanoplates. An ultrasonic shock wave can accelerate the Ostwald ripening processes and control the size of the as-prepared particles. Adsorption of poly(vinylpyrrolidone) (PVP) on different planes of silver nanoparticles induced the selective crystal growth of platelike structures. The products were characterized by X-ray powder diffraction (XRD), transmission electron microscopy (TEM), selected area electron diffraction (SAED), UV−vis spectroscopy, and atomic force microscopy (AFM). Structural characterization indicated that these platelike crystals were highly oriented single crystals with (111) planes as the basal planes. AFM images indicated that the average thickness of the as-prepared silver nanoplates was ca. 20 nm. The as-prepared silver nanoplates can be used as a template for the preparation of gold ringlike structures via a displacement reaction route. The as-prepared gold rings were also highly oriented single crystals and had the same morphologies as the silver nanoplates.

Experimental Section

All the reagents used were of analytical purity and were used without further purification. Silver nitrate, chloroauric acid, and *N*,*N*-dimethylformamide (DMF) were purchased from Shanghai Chemical Reagent Co. Ltd. (China). Poly(vinylpyrrolidone) (PVP-K30; MW 40000) was purchased from the Huakang Co. Chemical Reagent Factory (China). Distilled water was used in our experiments.

Silver nanoplates were synthesized by reducing $AgNO_3$ with DMF in the presence of PVP. In a typical synthesis, 20 mL of $AgNO_3$ solution (0.025M, in DMF) was added dropwise to a 20 mL PVP solution (0.005 M, in DMF). The mixture solution was exposed to high-intensity ultrasound irradiation under ambient conditions for 1/2 h. Ultrasound irradiation was accomplished with a high-intensity ultrasonic probe (Xinzhi Co., China, JY92-2D, 0.6 cm diameter; Ti-horn, 20 kHz) immersed directly into the reaction solution. The typical ultrasonic intensity was set as 60 W/cm^2. The product could be purified by centrifugation. In this case, the reaction mixture was diluted with water and centrifuged at 4000 rpm for 1/2 h. The products were characterized by XRD, TEM, SAED, AFM, and UV−vis spectroscopy.

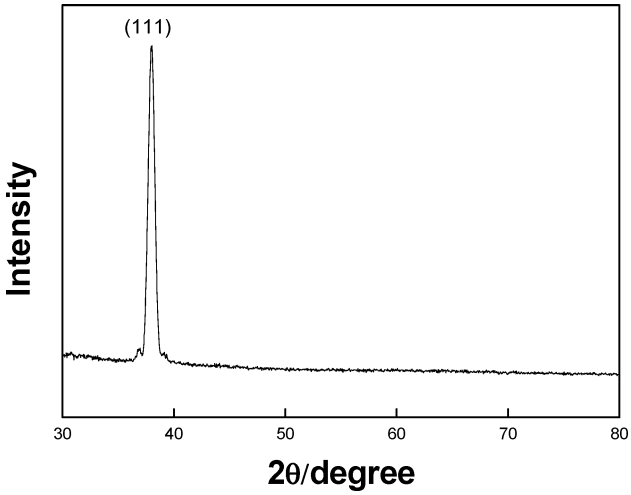

Figure 1. XRD pattern of the as-prepared silver nanoplates.

The XRD pattern was recorded using a Philp X'pert X-ray diffractometer. The TEM and SAED images were recorded on a JEOL JEM-200CX transmission electron microscope, using an accelerating voltage of 200 kV. The HRTEM images were recorded on a JEOL-4000EX transmission electron microscope, using an accelerating voltage of 400 kV. The AFM images (tapping mode) were recorded on an SPI 3800N atomic force microscope. The UV−vis absorption spectra were obtained using a SHIMADZU UV-3100 spectrophotometer.

Gold nanorings were prepared via a simple template method. In a typical synthesis, after the synthesis of silver nanoparticles was finished as mentioned above, a 0.0243 M $HAuCl_4$ solution of 6.7 mL was added dropwise into the hot solution under ultrasonic irradiation immediately (Au:Ag = 1:3), and the reaction was continued for 10 min. Then aqua ammonia solutions were added into the solution to dissolve the AgCl precipitate. After that, the products were centrifuged and washed with distilled water. The products were characterized by TEM and SAED. Different molar ratios of Au to Ag (1:4, 1:1) were also tried in the experiments.

Results and Discussion

Structural Characterization of Silver Nanoplates. Figure 1 is the typical powder XRD pattern of the as-prepared silver nanoplates. The overwhelmingly intensive diffraction located at $2\theta = 38.02°$ corresponds to the (111) lattice plane of a face-centered cubic (fcc) structure (JCPDS No. 4-0783), while peaks belonging to other lattice planes are quite weak. This indicates that (111) planes of silver nanoplates are highly oriented parallel to the supporting substrate. This structure feature is quite common for the metal nanoplates, such as silver,[4,8,17] gold,[9] copper,[10] and nickel[11] plates.

Figure 2a gives the TEM image of the as-prepared silver nanoplates with an average size of 120 ± 10 nm. Figure 2b is the SAED pattern of a single crystal. The set of spots with

(20) Maillard, M.; Huang, P.; Brus. L. *Nano Lett.* **2003**, *3*, 1611.
(21) He, R.; Qian, X.l Yin, J.; Zhu, Z. *J. Mater. Chem.* **2002**, *12*, 3783.
(22) He, R.; Qian, X.; Yin, J.; Zhu, Z. *Chem. Phys. Lett.* **2003**, *369*, 454.
(23) Susilck, K. S.; Cichowlas, A. A.; Grinstaff, M. W. *Nature* **1991**, *353*, 414.
(24) Didenko, Y. T.; McNamara, W. B.; Suslick, K. S. *J. Am. Chem. Soc.* **1999**, *121*, 5817.
(25) Suslick, K. S.; Price G. J. *Annu. Rev. Mater. Sci.* **1999**, *29*, 295.
(26) Pol, V. G.; Gedanken, A.; Calderon-Moreno, J. *Chem. Mater.* **2003**, *15*, 1111.

the strongest intensity could be indexed to (220) Bragg reflections with a lattice spacing of 1.44 Å, which indicates that the as-prepared nanoplates were single crystals with a (111) lattice plane as the basal plane. The inner set of spots with a lattice spacing of 2.50 Å was believed to originate from the 1/3 (422) plane normally forbidden by an fcc lattice, which suggested that the facets parallel to the TEM grid were smooth and flat. The appearance of the forbidden 1/3 (422) plane is often observed on silver or gold nanostructures in the form of thin plates or films bound by atomically flat and bottom faces.[4,6,17] Pileni et al.[27] suggested in their paper that (111) stacking faults existed in the platelike structures, which might be the reason for the occurrence of the 1/3 (422) forbidden reflections. The lattice constant calculated from this ED pattern was 4.066 Å, a value in agreement with the literature report of fcc silver ($a = 4.086$ Å). Figure 2d is the HRTEM image of the as-prepared nanoplates, and the fringe spacing is measured to be 0.25 nm, which corresponds well with the spacing between (422) planes of the fcc silver (0.250 nm). The flat structures were further confirmed by atomic force microscopy (tapping mode) as shown in Figure 3. Figure 3a is the two-dimensional image of silver nanoplates, and Figure 3b gives the three-dimensional image of a single silver nanoplate. The line analysis confirms the flatness of the top surface of the silver nanoplates with an average thickness of 20 nm.

Microscopic and Spectroscopic Monitoring of the Growth Process. Silver nanostructures at various stages of the growth process were characterized by TEM. Figure 4 shows the images of the sample taken from the reaction mixture after the solution was exposed to high-intensity ultrasound irradiation under ambient conditions for 0, 7, 9, and 20 min. In our experiments, DMF was used as a solvent and reducing agent. Liz-Marzan[28] had proposed the probable mechanism as follows:

$$HCONMe_2 + 2Ag^+ + H_2O \rightarrow 2Ag^0 + Me_2NCOOH + 2H^+ \quad (1)$$

Due to the quick reduction process, 2−5 nm spherical silver nanoparticles were formed immediately in the initial reaction mixture as shown in Figure 4a. At 7 min, a small spherical particle was still the main morphology; at the same time, a few 10−20 nm nanoprisms had appeared in the mixture (Figure 4b). These silver nanocrystals would serve as seeds for the growth of silver nanoplates. At 9 min, the reaction mixture became opaque; most particles in the mixture were 30−60 nm nanoprisms (Figure 4c), obviously larger than those at 7 min. After 20 min, the reaction was finished, and the main products were uniform triangular nanoplates (Figure 4d). The final products could be purified through careful centrifugation.

The growth process was also monitored by UV−vis absorption spectroscopy since silver nanostructures having different shapes exhibit surface plasmon resonance (SPR)

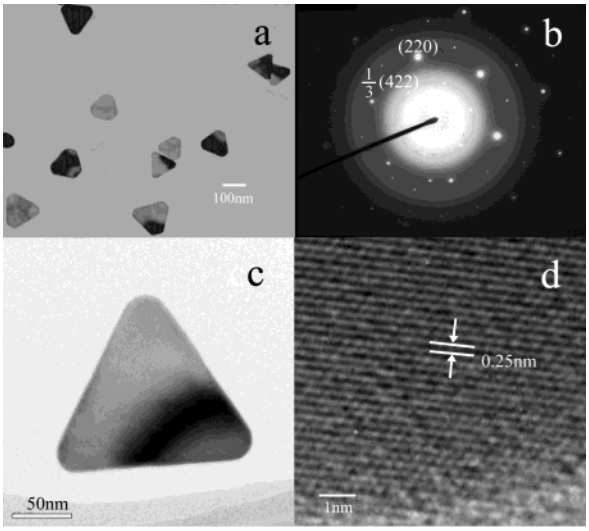

Figure 2. TEM, SAED, and HRTEM images of silver nanoplates: (a) TEM image of as-prepared silver nanoplates, (b) SAED image of silver nanoplates, (c) TEM image of a single crystal, (d) HRTEM image of silver nanoplates.

bands at different frequencies.[29,30] Figure 5 shows UV−vis spectra at different reaction stages. At the initial stage, there is a symmetric absorption peak centered at 416 nm, indicating the existence of small spherical silver nanoparticles. When the reaction was continued for 7 min, the symmetric absorption peak of spherical silver nanoparticles still existed, while another absorption peak centered at 495 nm appeared, showing the appearance of anisotropic silver nanostructures. When the reaction proceeded to 9 min, a peak centered at 538 nm appeared, accompanied by a much weaker absorption intensity at 416 nm, indicating the formation of polygonal structures of silver nanoparticles and the depletion of spherical silver nanoparticles. After the reaction was finished, three peaks at 653 nm (strong), 470 nm (medium), and 341 nm (weak) could be observed in the UV−vis spectrum of the as-prepared silver nanoplates. According to Mie's theory,[31] small spherical nanocrystals, either Ag or Au, should exhibit a single surface plasmon band, whereas anisotropic particles should exhibit two or three bands, depending on their shapes. Larger particles can exhibit additional bands corresponding to quadrupole and higher multipole plasmon excitation. On the basis of discrete dipole approximation, Jin et al.[4] gave theoretical calculation of the UV−vis spectroscopy of nanoprisms. According to Jin et al.,[4] for a perfect nanoprism, the 770 nm peak is the in-plane dipole plasmon resonance, the 470 nm peak is the in-plane quadrupole resonance, and the 340 nm peak is the out-of-plane quadrupole resonance. It was also mentioned[4] that the peak at 770 nm is very sensitive to the sharpness of the tips on the triangles. In this study, most of the nanoplates were also truncated; therefore, the 770 nm peak shifted to 653 nm.

The TEM observation and UV−vis absorption spectra described a clear growth process. The initial stage (before 7

(27) Germani, V.; Li, J.; Ingert, D.; Wang, Z. L.; Pileni, M. P. *J. Phys. Chem. B.* **2003**, *107*, 8717.
(28) Pastoriza-Santos, I.; Liz-Marzan, L. M. *Langmuir* **1999**, *15*, 948.
(29) Kerker, M. J. *Colloid Interface Sci.* **1985**, *105*, 297.
(30) Sarkar, D.; Halas, N. *J. Phys. Rev. E* **1997**, *56*, 1102.
(31) Mie, G. *Ann. Phys. (Leipzig)* **1908**, *25*, 377.

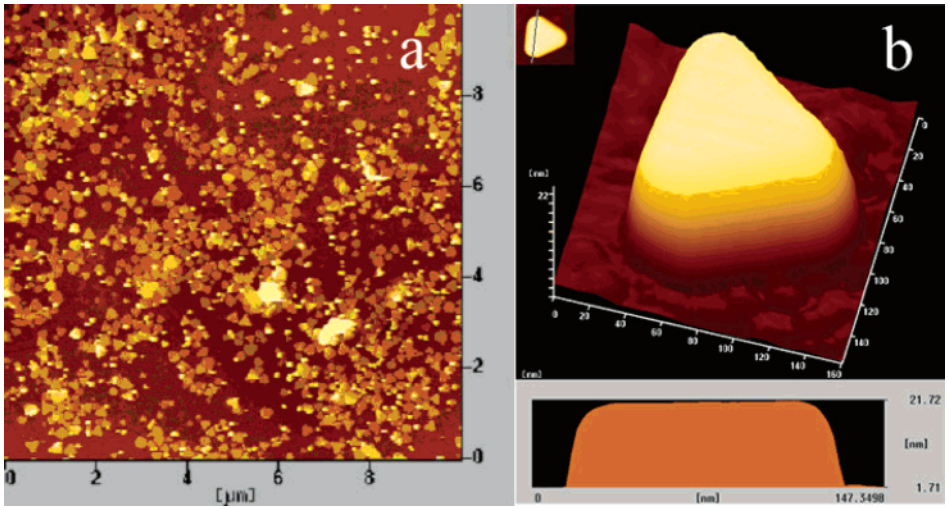

Figure 3. Atomic force microscopy image of the silver nanoplates: (a) two-dimensional AFM image of the silver nanoplates, (b) three-dimensional AFM image of a single silver nanoplate.

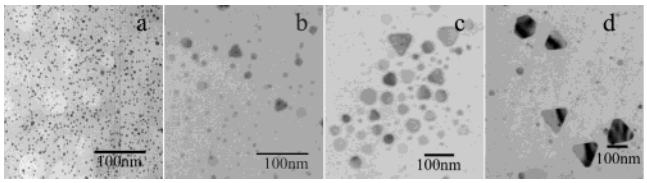

Figure 4. TEM images at different reaction times: (a) 0 min, (b) 7 min, (c) 9 min, (d) 20 min.

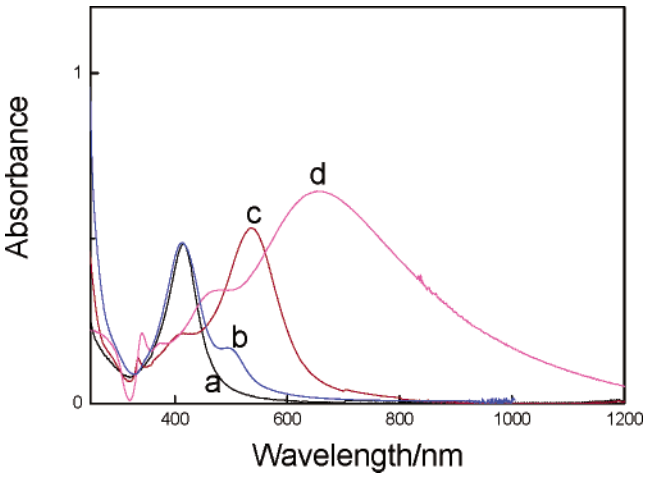

Figure 5. UV−vis spectra at different reaction times: (a) 0 min, (b) 7 min, (c) 9 min, (c) 20 min.

min) was a seed formation process, in which the size of the particles changes very slowly; at the medium stage (7−9 min), the seeds formed in the initial stage quickly grew to larger crystals via Ostwald ripening processes; after that, the growth rate gradually slowed. At last, after 20 min, the particles became stable. The average size of the particles at 20 min is the same as that at 30 min.

As the reaction proceeded, the amounts of initial particles decreased while plate-shaped crystals appeared and grew larger continuously. The silver nanoparticles of larger sizes were believed to grow at the expense of smaller ones via Ostwald ripening processes. In this process, small nanoparticles dissolved and grew into large crystals. The dissolution and crystal growth on the surface are the parallel processes. At the end of the reaction, the formation of uniform and well-shaped particles can be considered as a result of the balance between dissolution and crystal growth in the solvent. Due to the large surface-to-volume ratio of the nanosized particles, the dissolution is much easier; the growth rate is comparatively slower because small particles often grow much more slowly than macrocrystals.[32] Hence, the initial stage of the reaction was mainly a dissolution and prism-shaped seed formation process. After a certain time of dissolution, the supersaturated Ag began to promote the crystal growth on the surface of the seeds. The crystal growth reached the maximal rate in a very short time, and then the rate decreased gradually. The above growth process corresponds well with the UV−vis absorption spectra.

This kind of silver nanoplate was first synthesized in the same solvent using a heating method.[5] In the thermal process, the formed nanoprisms become larger with time, and a wider variety of shapes are found for longer boiling times.[5] However, in our experiments, the prepared particles became stable with uniform shape after 20 min. The kinetics of ultrasonic degradation is different from those of thermal processes. In the sonication process, cavitation bubble collapse will launch shock waves into the liquid. The large forces from the waves can even result in the breakage of the bonds in the polymer chain. When these shock waves pass over particles, they can also cause the rapid impact of the liquid on the surface of the particles and promote the dissolution of the small particles.[25] The strong impact from the shock waves was more effective in accelerating the Ostwald ripening processes.

Influence of the Ultrasonic Intensity and the Molar Ratio between PVP and $AgNO_3$. The sonication effects were further proved by the changes in sizes of the as-prepared silver nanoparticles under different ultrasonic intensities. The silver nanoplates had an average size of 100 ± 20 nm (Figure 6a) when the reaction was under a lower ultrasonic intensity (55 W/cm^2); the average size of the nanoplates increased to

(32) Mullin, J. W. *Crystallization*, 3rd ed.; Butterworth Heinemann: Woburn, MA, 1997; pp 172−202.

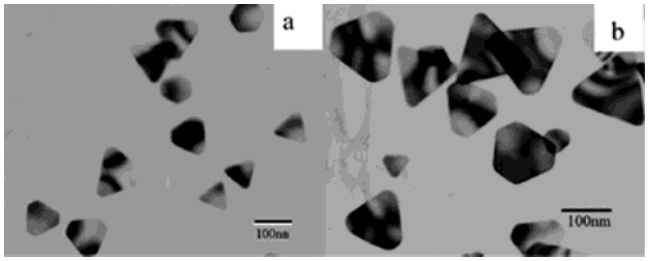

Figure 6. TEM images of the silver nanoplates prepared under different ultrasonic irradiation intensities: (a) 55 W/cm^2, (b) 65 W/cm^2.

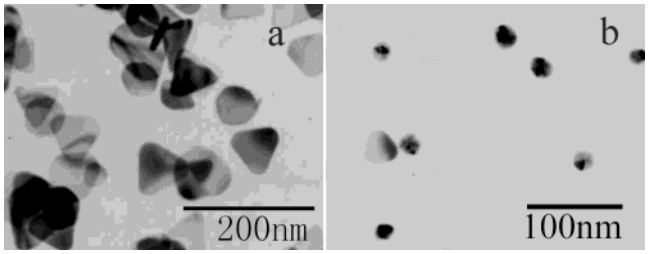

Figure 7. TEM images of as-prepared products, showing the variation of morphology when the molar ratio between PVP and $AgNO_3$ was changed: (a) $n_{PVP}/n_{AgNO_3} = 0.025$, (b) $n_{PVP}/n_{AgNO_3} = 0.5$.

120 ± 10 nm (Figure 4a) when the reaction was under a medium ultrasonic intensity (60 W/cm^2); as the ultrasonic intensity increased to 65 W/cm^2, the average size increased to 150 ± 20 nm (Figure 6b). Since the temperature of the reaction mixture under different ultrasonic intensities remains constant, the difference of sizes only comes from the changes of the ultrasonic intensity. According to TEM images, the final products had a larger crystal size under a higher ultrasonic intensity. As was mentioned before, silver crystals grow to be a larger size at the expense of small crystals via ultrasonic-assisted Ostwald ripening processes. Higher ultrasonic intensity would induce more cavitation bubble collapse and a stronger shock wave, which can accelerate the dissolution of the small crystals more quickly. Since the formation of the stable particles can be considered as a result of the balance in Ostwald ripening processes, the difference in the particle sizes might also be considered as a result of the changes in this kind of balance. By changing the ultrasonic intensity, we can control the size of the particles.

Otherwise, the morphology of the silver nanoplates strongly depended on the molar ratio of PVP and $AgNO_3$. Figure 7 shows the TEM images of as-prepared silver nanoplates under different molar ratios.

The molar ratio of PVP and $AgNO_3$ between 0.1 and 0.3 favored the growth to the triangular silver nanoplates. When the ratio was reduced, the as-prepared silver nanoplates had more round corners, and some particles had polyhedral structures. Figure 7a shows the morphology of a sample when the molar ratio was 0.025. Higher molar ratios between PVP and $AgNO_3$ were also tried; however, in that case, the crystals were surface coated with a thick PVP layer. As a result, small spherical or polyhedral silver crystals were the main products (Figure 7b), indicating that a large amount of PVP was unfavorable for the growth of silver nanoplates.

The observed growth patterns suggest that the presence of PVP induced the formation of triangular silver particles. El-sayed et al.[33] provided two reasonable explanations for the formation of faceted particles: (1) the growth rates vary at different planes of the particles; (2) particle growth competes with the coordinating action of stabilizers. During the course of the preparation of nanocrystals, small molecules or polymers are often used which selectively adsorb on certain crystal planes and induce anisotropic growth of different planes. Ag,[4,6−8] Au,[9] Cu,[10] Pd, and Ni[11] triangular or hexagonal plates have been prepared with this method. In the present study, PVP was used as a stabilizer, which might kinetically control the growth rates of various faces by interacting with these faces through adsorption and desorption.

Since the (111) planes were the basal planes of the prepared silver nanoplates, the growth at the edges of the nanoplates should be along the (100) or (110) direction. In our Ag/PVP system, the selective adsorption of PVP obviously slows the growth rate on the (111) plane. At the favorite molar ratio, the plates are elongated along the (100) and (110) directions. At the lower molar ratio, two factors influence the formation of the triangular plates: (1) due to the less selective absorption, the equivalent growth rate on different planes induced the formation of a polyhedral structure; (2) without the protection of the surfactant, the strong shock wave will cause high-velocity interparticle collisions, especially removing the surface material at the angles and smoothing the particles.[25] At a much higher molar ratio, the excessive absorption will limit the growth rate on all planes; on the other hand, the equivalent growth rate also induced the polyhedral structure.

Preparation and Characterization of Gold Nanorings. Gold nanorings have been prepared via a simple template method. Because the standard reduction potential of the $AuCl_4^-$/Au redox pair (0.99V vs SHE) is higher than that of the Ag^+/Ag redox pair (0.80V vs SHE), silver nanoparticles can be oxidized to silver ions immediately when $HAuCl_4$ solution is added to the solution.

$$3Ag + AuCl_4^- \rightarrow Au + 3AgCl + Cl^- \qquad (2)$$

The AgCl precipitate can be removed by aqua ammonia. Figure 8 is the XRD pattern of the gold ringlike structure. The overwhelming intensive diffraction was also located at $2\theta = 38.02°$, which corresponds to the (111) lattice plane of fcc gold, indicating that the as-prepared gold rings are highly oriented with the (111) plane parallel to the supporting substrate. Figure 9a is the TEM image of monodisperse gold rings. These gold nanorings have morphology similar to that of silver templates. The SAED image indicates that the nanorings are single crystals and can be indexed to fcc gold. According to the HRTEM image, the fringe spacing is calculated to be 0.25 nm, which is in good accord with the spacing between forbidden 1/3 (422) planes of fcc gold (0.250 nm).

Different molar ratios between gold and silver can lead to different morphologies, which may help in understanding

(33) Petroski, J. M.; Wang, Z. L.; Green, T. C.; El-Sayed, M. A. *J. Phys. Chem. B* **1998**, *102*, 3316.

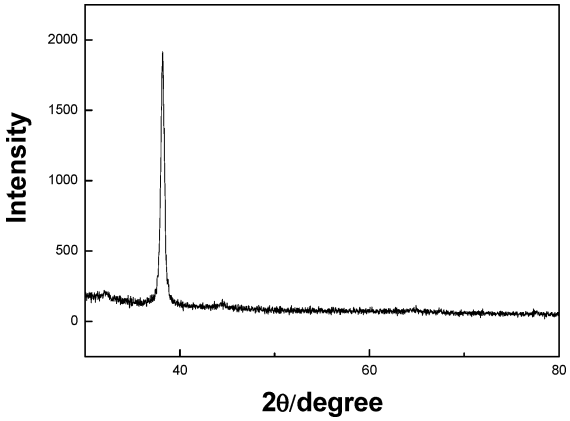

Figure 8. XRD pattern of the prepared gold nanorings.

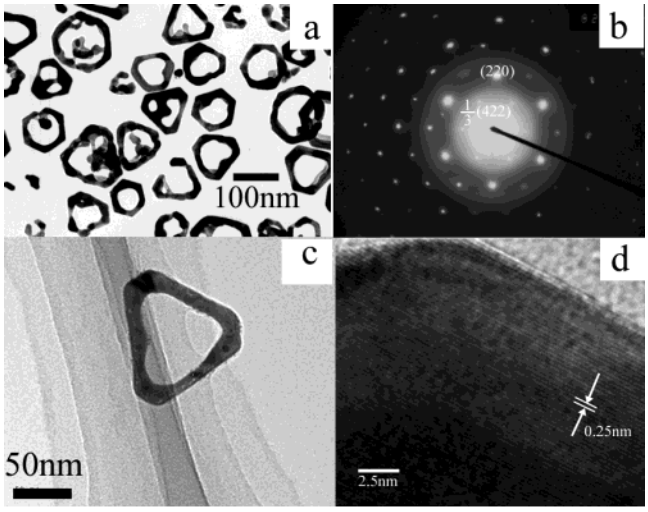

Figure 9. TEM, SAED, and HRTEM images of a gold nanoring: (a) TEM image, (b) SAED image, (c) a single gold nanoring, (d) HRTEM image.

the formation of ringlike structures. According to the literature,[7,34] the free energies associated with the crystallographic planes of an fcc metal decrease in the order $\gamma_{(110)} > \gamma_{(100)} > \gamma_{(111)}$; therefore, the displacement reaction will occur on the surface of a silver nanoplate in the order (110), (100), (111). Because the as-prepared silver nanocrystal has the (111) lattice plane as the basal plane, the displacement reaction mainly occurred along the faceted edges of the plates to form a ringlike structure of gold crystal around the silver template first, and then the chloroauric acid began to displace central silver atoms to form a gold slice on the surface of the (111) plane.[19] Meanwhile, the gold on the surface also dissolved into the solvent continually under the ultrasound irradiation. Since the dissolution rate of the gold on the (111) plane was much quicker than the crystal growth rate, the gold slice was replaced to the faster growing faces via Ostwald ripening processes. Thus, in this process, the gold at the edges would serve as nuclei and grow to the gold nanorings finally. When the molar ratio between Au and Ag was 1:4, which was lower than the stoichiometric ratio (1:3) shown in eq 2, the as-prepared nanoparticles had ring structures with a thin layer of silver (111) planes (Figure 10a). Since this thin layer was only observed in products whose molar ratio was lower than the stoichiometric ratio, we believed that the layer was composed of silver atoms on the (111) plane that had not been displaced yet. When the molar ratio was greater than or equal to the stoichiometric ratio, as is shown in Figure 10b,c, the central atoms completely disappeared and the final products had ringlike structures.

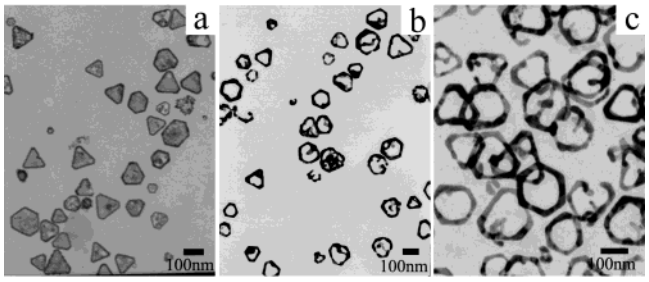

Figure 10. TEM images of prepared nanorings with different gold/silver ratios: (a) Au:Ag = 1:4, (b) Au:Ag = 1:3, (c) Au:Ag = 1:1. The ultrasonic intensity was set as 65 W/cm^2.

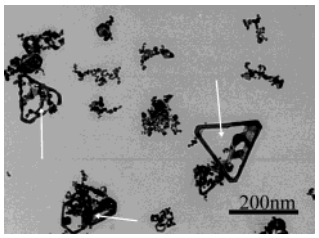

Figure 11. TEM image of prepared nanorings under 30 W/cm^2 ultrasonic intensity.

As we mentioned before, the Ostwald ripening processes were enhanced by ultrasonic irradiation. In the replacement process from the silver nanoplates to the gold nanorings, the ultrasonic irradiation also plays an important role. We have tried the synthesis of gold nanorings under different ultrasonic intensities, which might help to explain the effects of ultrasonic irradiation. Under a lower ultrasonic intensity (30 W/cm^2), there are a lot of broken pieces of gold nanocrystals observed in the TEM image (Figure 11) when the reaction was continued for 10 min. When the ultrasonic intensity is 60 W/cm^2, only very few broken pieces occur in the products. We suppose the pieces come from the Au on the (111) plane of the nanoplates (the areas indicated in Figure 11). Since the Ag is easily replaced by Au, the replacement reaction takes place very quickly. Under high ultrasonic intensity, the sonication will promote the Ostwald ripening processes and the Au on the (111) plane will be transferred to the frameworks. Under low ultrasonic intensity, the effect of Ostwald ripening processes is relative weak and the Au will soon form many Au islands on the (111) plane. These islands are unstable under ultrasound irradiation and will break into many pieces as we observed in the TEM image.

Conclusion

A simple and effective route has been developed for the preparation of 2D structures such as silver nanoplates and gold nanorings. Silver nanoplates were prepared via a sonochemical method. The as-prepared silver nanoplates

(34) Wang, Z. L. *J. Phys. Chem. B* **2000**, *104*, 1153.

were uniform and highly oriented single crystals with (111) planes as the basal planes. These platelike nanocrystals could serve as templates to fabricate ringlike metal structures via a simple displacement reaction under ultrasonic irradiation. The as-prepared gold nanorings have the same morphology as silver nanoplates and are also highly oriented single crystals. We studied the reaction mechanism and proposed a PVP-assisted selective and ultrasonic-enhanced growth process. The prepared silver nanoplates and gold rings could be oriented on the surface of the substrate and might help to explore new applications in the direct electrochemistry of biomolecules such as horseradish peroxidase in the future.

Acknowledgment. This work is supported by the National Natural Science Foundation of China (Grant No. 20325516 and 90206037) and the Research Foundation for the Doctoral Program of the Ministry of Education of China (Grant 20020284022). We are grateful to Dr. Lin Pu from the Department of Physics and Prof. Xiangkang Meng from the Department of Materials Science and Engineering for their sincere help. We also thank Mr. Jianming Hong from the Modern Analytic Center at Nanjing University for extending his facilities to us.

IC049529D